Modeling a Photovoltaic Emulator Using Four Methods and Buck-Boost Converter

S.Jenkal*, M.Kourchi, A.Rachdy, O.Oussalem, M.Ajaamoum and M.Oubella

Abstract—**This work is devoted to the synthesis results of the current-voltage characteristic performances obtained by four modelling methods. The aim these models is to emulate the current-voltage characteristics of a photovoltaic module using DC-DC Buck-Boost converter. The first class of the developed methods is based on physical properties. It takes into account the output current of the electrical circuit. The second class uses a system of polynomial equations. It is based on multiple straight lines. The mathematical models are built and validated by a simulation using MATLAB/SIMULINK. The comparative study of the four models demonstrated the performances of the models under study.**

Index Terms— **Emulator, Buck-Boost converter, Photovoltaic system, Mathematical Modelling.**

I. INTRODUCTION

Photovoltaic solar energy represents an inexhaustible source of green energy and alternative to fossil fuels.[1] This energy is more and more applied in various fields going from the residential and commercial installations to the space systems, thanks to many advantages; It is noiseless, easy to install, and requires a short construction period.[2][3][4]

The very high rate of growth of the photovoltaic (PV) industry makes the availability of specialized equipment for laboratory tests becoming crucial. In particular for manufacturers and laboratories working in the field of power electronics, linked to PV installations. [5][6][7].

The results obtained require validation by appropriate experiments involving the PV source as well as various types of loads, such as resistive loads, DC motors and accumulators.

S.Jenkal is a PhD candidate of the laboratory of engineering sciences and energy management (LASIME), in the national school of applied sciences (ENSA), Agadir, Morocco (email: samia.jenkal@edu.uiz.ac.ma).

M.Kourchi is a Professor and researcher at High School of Technology, Morocco (email: m.kourchi@uiz.ac.ma).

A.Rachdy is a Professor and researcher at High School of Technology, Morocco (email: a.rachdy@uiz.ac.ma).

O.Oussalem is a PhD candidate of LASIME, in the national school of applied sciences (email: otman.oussalem@edu.uiz.ac.ma).

M.Ajaamoum is a Professor and researcher at High School of Technology, Morocco (email: m.ajaamoum@uiz.ac.ma).

M.Oubella is a Professor and researcher at High School of Technology, Morocco (email: m.oubella@uiz.ac.ma).

Therefore, the photovoltaic emulator facilitates the experimental analysis of photovoltaic systems [8], [9]. It is based on the modeling of photovoltaic sources and offers transportability, independence from weather conditions and ease of use.

However, the proper functioning of these emulators depends on the quality of the mathematical models used to represent the photovoltaic generators. The choice of these models directly affects the static and dynamic performance of the photovoltaic emulator [10][11][12].

In practice, there are two major types of PV models. The electrical circuit model and the interpolation model[13][14][15].

The electrical circuit model, also known as the analytical model[16][17], is a modeling based on the equivalent circuit of a solar cell and the equation of the current-voltage characteristics is defined using the Kirchhoff current law[18].

The interpolation model allows replacing the current-voltage curve by another one, that is simpler. The new curve is based on multiple straight lines, and coincides with the first at a finite number of points given at the start. There are various types of interpolation models used in the PV emulator [8][19][20].

In this context, the work we have carried out aims to develop models that reproduce the current-voltage characteristic with high accuracy regardless of temperature and irradiance conditions. These models will serve as a control stage of photovoltaic panel emulators. The study is based on a comparison of four models: "five parameter model", "four parameter model", "five lines model" and "two lines model".

The rest of this paper is arranged as follows: Section 2 provides a description of the PV emulator that have been developed. Methodology and simulation are presented and explained in Section 3. Results and discussions are given in Section 4. And finally, a conclusion is presented in Section 5.

II. METHODOLOGY

A. System description

Figure 1 presents an overview of the proposed system. It consists a sensor circuitry and a microcontroller connected to a Buck-Boost converter. The converter is piloted by a control unit that is built in MATLAB/SIMULINK using mathematical models to reproduce the I-V characteristics of a PV module.
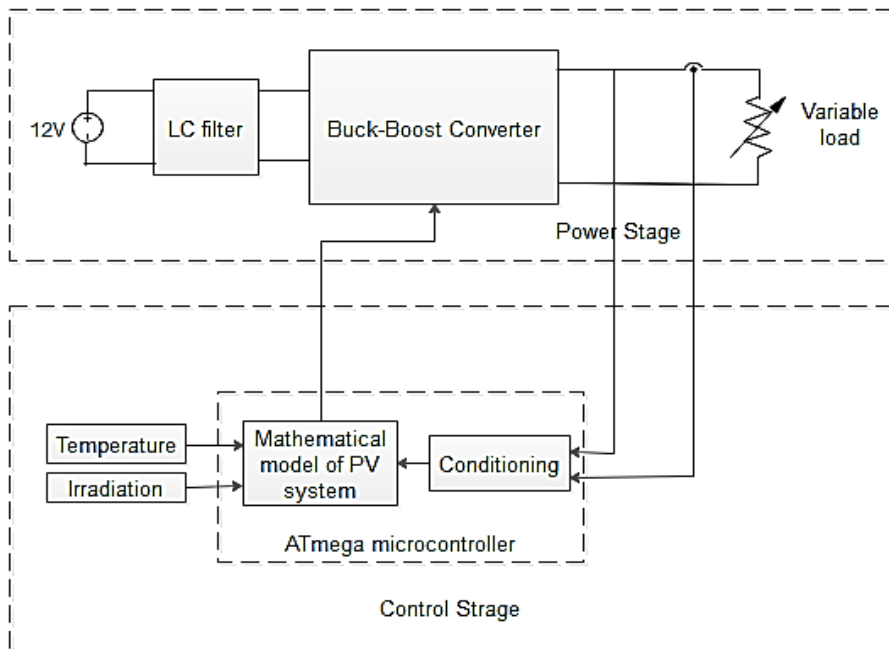
Fig. 1. Overview of the proposed system.

A. Electrical circuit model

The PV cells are considered the smallest elements of a photovoltaic module[21]. They convert directly, solar irradiation to electricity by the photovoltaic effect. In fact, different models have been developed to represent the electrical output of photovoltaic modules. These simplified models are defined as: ideal model, simple diode model and two diode model [22],[23]. In the present work, the simple diode model is analyzed due to the simplicity of this model and its accuracy.

The single diode model, shown in Fig. 2, is an electrical model based on series resistor and a shunt resistor. The latter can be simplified by neglecting the shunt resistance as shown in Fig. 3.

Single Diode Model

The single diode model takes into account series resistance (R_s) and shunt resistance (R_p), which affect the illuminated current–voltage (I–V) characteristics and efficiency of cells. It represent the simple equivalent electrical circuit of a real solar cell [24].

Where:
I_{ph}: Photocurrent.
I_0: Reverse saturation current for an ideal pn-junction diode.
A: Ideality factor of the solar cell.
$V_t = N_s KT / q$: thermal voltage.
N_s: Number of cells connected in series.
K: Boltzmann's constant (1.38 10-23 J / K).
T: Real junction temperature (K).
q: Elementary charge.
R_s: Series resistance (Ω).
R_p: Shunt resistance (Ω).

Single Diode Model with Rs

The single diode model with Rs has been developed to describe the electric circuits in series with the photovoltaic cell, that exists in reality and have a certain electric resistance. It is more accurate than the ideal one, but it is not a comprehensive one since the series resistance R_s is quite low whereas the shunt resistor R_p is relatively high, then the current I_{ph} consumed by R_p is miniscule, which leads to neglect the effect of this resistance R_p [24]
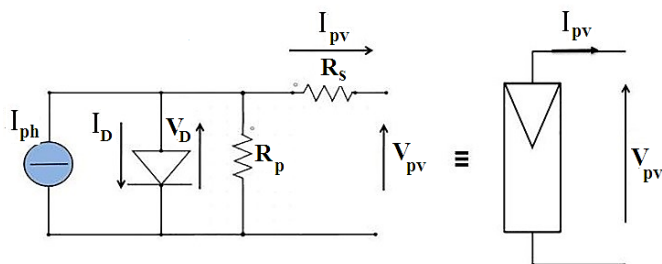

Fig. 2. Equivalent circuit of a solar cell with Rs and Rp.

According to Figure 2, the output current of the model is described as follows:

$$I_{ph} - I_0\left[\exp\left(\frac{V_{pv} + R_s I_{pv}}{AV_t}\right) - 1\right] - \frac{V_{pv} + R_s I_{pv}}{R_p} - I_{pv} \quad (1)$$
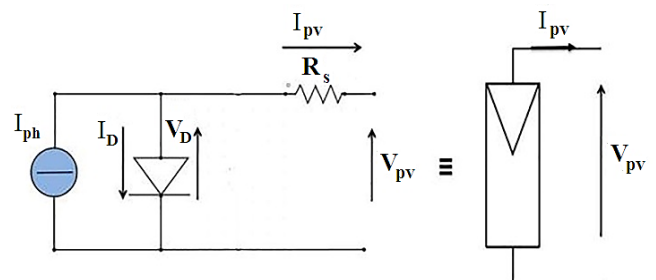

Fig. 3. Equivalent circuit of a solar cell with Rs.

According to Figure 3, the output current of the model is described as follows:

$$I_{pv} - I_{ph} + I_0 \left[\exp\left(\frac{V_{pv} + R_s I_{pv}}{A V_t} \right) - 1 \right] = 0 \quad (2)$$

Five Parameter Model

The equation 1 is an implicit equation, there is I_{pv} and V_{pv}. To solve this equation the iterative numerical methods can be used. In this paper, we chose the Newton/Raphson method. It is a powerful technique for solving equations numerically. This equation has five parameters (I_{ph}, I_0, A, R_s and R_p). However, the identification of these five parameters requires the resolution of 5 equations. For this resolution, we perform an analysis of equation 1 around the three remarkable points on curves I_{pv} (V_{pv}): the open circuit point V_{oc}, the maximum power point P_{max} and the short circuit point I_{sc}. The equations obtained by this analysis are independent and sufficient for the determination of the five parameters that we represent in vector form:

$$F(p) = \begin{bmatrix} I_{ph-I_0}\left[\exp\left(\frac{V_{oc}}{AV_t}\right)-1\right]\frac{V_{oc}}{R_p} \\ I_{ph} - I_0\left[\exp\left(\frac{R_s I_{sc}}{AV_t}\right)-1\right]\frac{R_s I_{sc}}{R_p} - I_{sc} \\ \frac{-I_0}{AV_t}\left(1-\frac{R_s}{R_{s0}}\right)\exp\left(\frac{V_{oc}}{AV_t}\right)-\frac{1}{R_p}(1-\frac{R_s}{R_{s0}})+\frac{1}{R_{s0}} \\ \frac{-I_0}{AV_t}\left(1-\frac{R_s}{R_{p0}}\right)\exp\left(\frac{R_s I_{sc}}{AV_t}\right)-\frac{1}{R_p}(1-\frac{R_s}{R_{p0}})+\frac{1}{R_{p0}} \\ \frac{-I_0}{AV_t}\left(1-\frac{I_{mpp}R_s}{V_{mpp}}\right)\exp\left(\frac{V_{mpp}+I_{mpp}R_s}{AV_t}\right)-\frac{1}{R_p}(1-\frac{I_{mpp}R_s}{V_{mpp}})+\frac{I_{mpp}}{V_{mpp}} \end{bmatrix} \quad (3)$$

To resolve the function F (P) = 0 we used the function "Fsolve" which is based on the Levenberg-Marquardt method [25]. P_0 is the first value of the parameter matrix. It allows calculating the first solution P_1. The resolution program is performed iteratively, and displays the parameters if the stopping criterion is reached. Otherwise, it takes P_1 as a first new value of the parameter matrix and restarts the calculation program.

To accelerate the convergence of the iterative program, we have been able to determine the initial values of the parameters (I_{ph}, I_0, R_s, R_p, A) according to the following equations:

$$R_{s0} = \frac{dV}{dI}\bigg|_{\substack{V=V_{oc} \\ I=0}} \quad (4)$$

$$R_{p0} = \frac{dV}{dI}\bigg|_{\substack{V=0 \\ I=I_{sc}}} \quad (5)$$

$$A = \frac{2V_{mppn} - V_{con}}{V_{tn}\left[\frac{I_{ccn}}{I_{ccn}-I_{mppn}}+\ln\left(1-\frac{I_{mppn}}{I_{ccn}}\right)\right]} \quad (6)$$

$$I_0 = \left(I_{sc,n} - \frac{V_{oc,n}}{R_p}\right)\exp\left(-\frac{V_{oc,n}}{AV_{t,n}}\right) \quad (7)$$

$$I_{ph} = I_{sc,n}\left(1 + \frac{R_s}{R_p}\right) + I_0 \exp\left(-\frac{V_{oc,n}}{V_{t,n}}\right) \quad (8)$$

The resolution of the function F (P) = 0 gives the following values:

$I_o = 6{,}67 \times 10^{-16}$ (A)

$I_{ph} = 3.999$ (A)

$A = 0.6345$

$R_s = 0.6409$ (Ω)

$R_p = 148{,}4753$ (Ω)

After the identification of these five parameters, the equation (1) is solved using the Newthon-Raphson method. The algorithm is based on the Taylor development, the equation (1) is linearized at $I_{pv,k}$, and the next point ($I_{pv,k}+1$) is calculated iteratively according to the equation (9).

The expression of the stop criterion of the iterations is shown in equation (10) giving ε = f (I_{pv}, V_{pv}) which represents the value of equation (1) with the current $I_{pv\,(k+1)}$ which is expressed by:

$$I_{pv;k+1} = \frac{I_{ph} - I_0\left[\exp\left(\frac{V_{pv}+R_s I_{pv,K}}{AV_t}\right)-1\right] - \frac{V_{pv}+R_s I_{pv,K}}{R_P} - I_{pv,k}}{-I_0\frac{R_s}{AV_t}\exp\left(\frac{V_{pv}+R_s I_{pv,k}}{AV_t}\right)-\frac{R_s}{R_p}-1} \quad (9)$$

$$\varepsilon = I_{ph} - I_0\left[\exp\left(\frac{V_{pv}+R_s I_{pv,K+1}}{AV_t}\right)-1\right] - \frac{V_{pv}+R_s I_{pv,K+1}}{R_P} - I_{pv,k+1} \quad (10)$$

Four Parameter Model

In order to identify the parameters we used a "Slope method" technique at the point (V_{oc}, 0). This model uses the fact that the series resistance influences the slope of the (current-voltage) characteristic curve next to the point (V_{oc}, 0). The purpose of this identification method is to explicitly determine the four parameters I_{ph}, I_0, A, R_s.

The photo-current I_{ph} is depending on the real irradiation level G and the real junction temperature T according to equation (11):

$$I_{ph} = I_{ph,n}\left(\frac{G}{G_n}\right)\left[1 + K_i(T - T_n)\right] \quad (11)$$

We obtain the following set of equations used to identify the unknown parameters:

$$I_0 = I_{ph}\exp\left(\frac{-V_{co}}{AV_t}\right) \quad (12)$$

$$A = \frac{2V_{mpp,n} - V_{co,n}}{V_{t,n}\left[\frac{I_{scn}}{I_{sc,n}-I_{mpp,n}}+\ln\left(1-\frac{I_{mpp,n}}{I_{sc,n}}\right)\right]} \quad (13)$$

$$R_s = \frac{dV}{dI}\bigg|_{\substack{v\infty \\ I=0}} - \frac{1}{\frac{I_0}{AV_t}\exp\left(\frac{V_{co}}{AV_t}\right)} \quad (14)$$

Where:
G: Real Irradiance level (W/m²).
G_n: STC irradiance levels (W/m²).
T_n: Nominal temperature (K).
Ki: Temperature coefficient of the short-circuit

After the identification of these four parameters, the equation (2) is solved using the Newthon-Raphson method as the previous 5-parameter model, eliminating the terms containing R_p, which is expressed by:

$$I_{k+1} = \frac{I_{ph} - I_0 \left[\exp\left(\frac{V + R_s I_K}{AV_t} \right) - 1 \right] - I_k}{-I_0 \frac{R_s}{AV_t} \exp\left(\frac{V + R_s I_k}{AV_t} \right) - 1} \quad (15)$$

$$\varepsilon = I_{ph} - I_0 \left[\exp\left(\frac{V + R_s I_{K+1}}{AV_t} \right) - 1 \right] - I_{k+1} \quad (16)$$

B. Multiple Straight Lines Models

In these models, we calculate N points of the I-V characteristic by using a system of polynomial equations [26]. Then, by these points, we will be able to calculate the other points of the I-V characteristic of the panel using the linear interpolation.

Two Lines Approach

In this approach, we calculate three points of the (current-voltage) characteristic [13]. Then, by these points, we calculate the rest of the current-voltage characteristic points. The two ends of the curve present the short-circuit current (0V, I_{sc}) and the open-circuit voltage (V_{oc}, 0A). The last point (V_{mpp}, I_{mpp}), is the point with the maximum power (MPP). The three points are calculated according to the following equations:

$$\begin{cases} V_{mp} = V_{mp,n} + V_t \times \log\left(\frac{G}{G_n} \right) + Kv \times (T - T_n) \\ I_{sc} = I_{sc,n} \times \left(\frac{G}{G_n} \right) + K(ci \times (T - T_n)) \\ I_{mp} = I_{mp,n} \times \left(\frac{G}{G_n} \right) + (Ki \times (T - T_n)) \end{cases} \quad (17)$$

Five Lines Approach

In this approach, we need to select six points from the curve to generate five fitting lines. Basically, the two ends points of the five lines curve present the short-circuit current (0V, I_{sc}) and the open-circuit voltage (V_{oc}, 0A). The third point is the maximum power point (MPP) of the curve. Then, we select three other points: ((V_{oc} + V_{mpp})/2, I_3), (V_2, I_2), (V_{oc}/2, I_1) to improve the precision of the current-voltage curve.

As shown in equation (18), we get by the six points, five lines:

$$\begin{cases} V_{oc} = c_0 + c_1 \ x_2 + c_2 \ x_3 \\ V_{mp} = c_0 + c_1 \ x_3 + c_2 \ x_2 + c_3 \ x_1 \ x_3 \\ I_{sc} = c_1 \ x_1 + c_2 \ x_2 \\ I_1 \ = c_1 \ x_1 + c_2 \ x_2 + c_3 \ x_1 \ x_2 \\ I_2 \ = c_0 + c_1 \ x_1 + c_2 \ x_2 + c_3 \ x_1 \ x_2 \\ I_{mp} = c_0 + c_1 \ x_1 + c_2 \ x_2 + c_3 \ x_1 \ x_2 \\ I_3 \ = c_1 \ x_1 + c_2 \ x_1^2 + c_3 \ x_1 \ x_2 + c_4 \ x_1^2 \ x_2 \end{cases} \quad (18)$$

c_0, c_1, c_2, c_3 and c_4 are the Interpolation coefficients ensuring a good smoothing.

In these equations x_1, x_2 and x_3 present the functions of temperature T and radiation G, according to the following equations:

$$\begin{cases} x_1 = \frac{G}{G_n} \\ x_2 = T - Tn \\ x_3 = \log_{10}(G/Gn) \end{cases} \quad (19)$$

Buck-Boost converter

A DC-DC Buck-Boost is used to minimize the input voltage. In our case, the converter can emulate a panel with V_{oc} that goes to 30V with a 6V voltage.

The sizing of the converter was based on the literature [24] with a configuration that allows to replicate the characteristics of the selected solar PV panel. The switching frequency of the Buck-Boost converter is 33 kHz with V_{in}= 6V. The values of L and C used after the sizing are L=1.49mH and C=1,23mF.

To limit the ripple effect of the voltage and the current at the load, we added a low-pass filter LC.

The schematic diagram of the Photovoltaic emulator based on the DC-DC converter are coded and executed in the Matlab environment as shown in figure (4):

III. RESULTS AND DISCUSSION

In this section, we expose and discuss the performance of the PV emulator and the obtained measurements, for the different types of approaches:

The results are validated through the datasheet of PV panel Solarex MSX-64. Tables 1 summarize the electrical characteristics of the panel under study.

TABLE I
TYPICAL ELECTRICAL CHARACTERISTICS OF MSX-64: 25 ℃, AM 1.5, 1000 W/M2

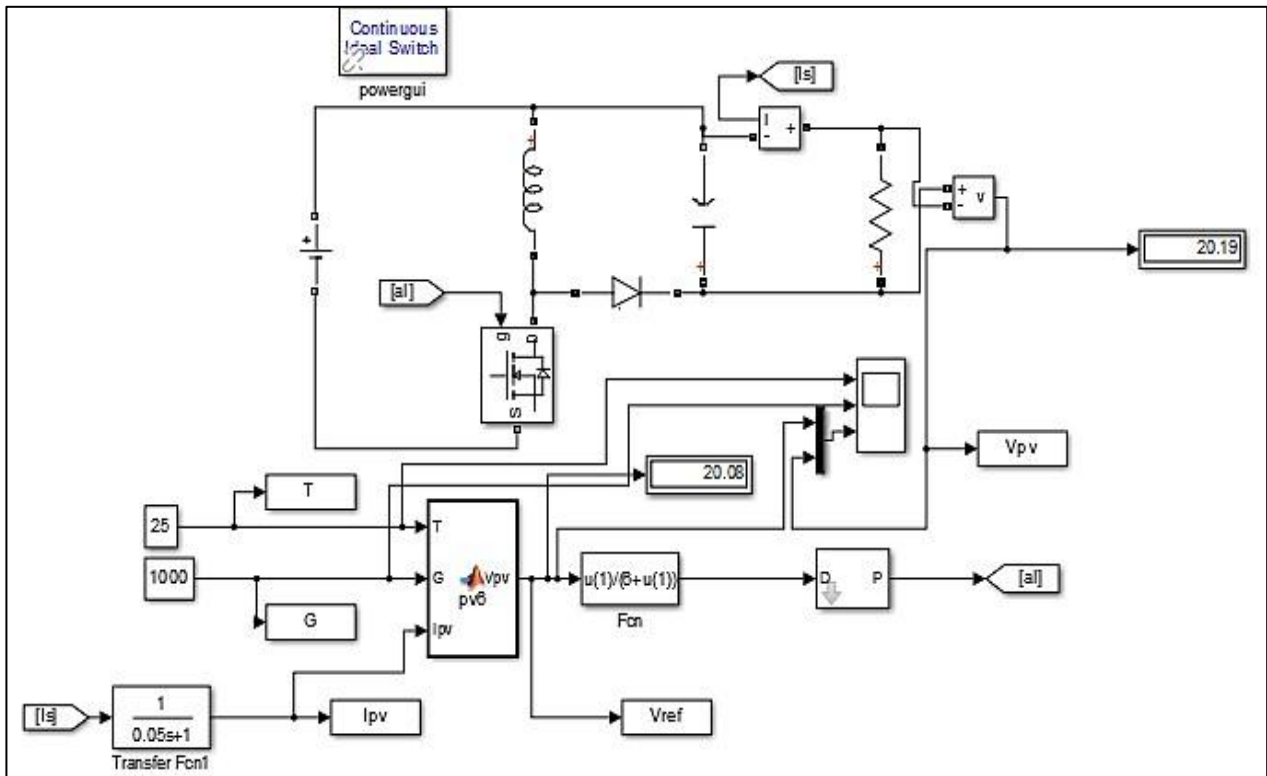| Parameter	Value
Current at maximum power (I_{mp})	3.66 A
Voltage at point of maximum power (V_{mp})	17.5 V
Cell number (Ns)	36
Nominal open-circuit voltage (V_{ocn})	21.3 V
Nominal short-circuit (I_{SCN})	4.0144 A
Kv temperature coefficient of the voltage circuit open	0.074107
Ki temperature coefficient of the short circuit	0.004832

Fig. 4. The developed PV emulator based on different models in Matlab / Simulink..

Fig. 5. Comparison between datasheet and five parameter model results on emulator
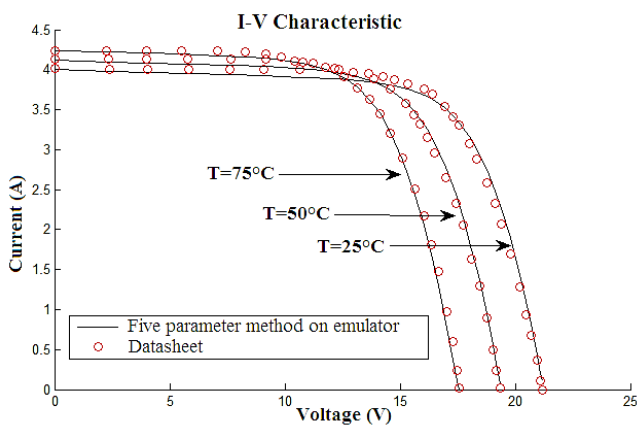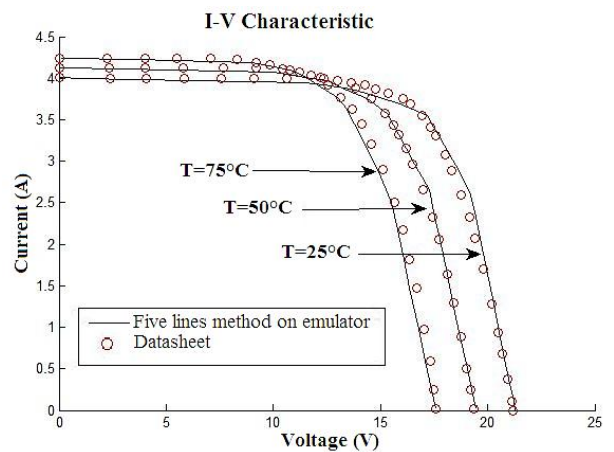

Fig. 6. Comparison between datasheet and four parameter model results on emulator

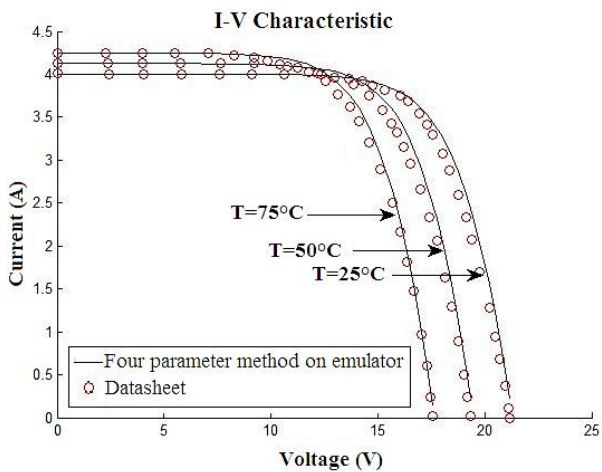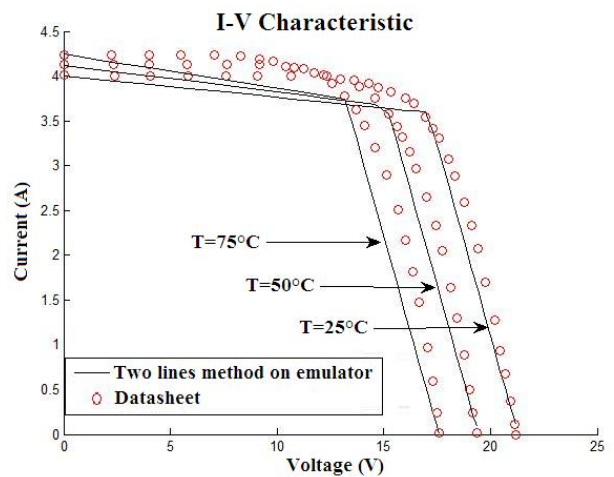Fig. 7. Comparison between datasheet and five lines model results on emulator

Fig. 8. Comparison between datasheet and two lines model results on emulator

Figures 5, 6, 7, 8, expose the results of the different models on the PV emulator, compared to the datasheet curves given by the manufacturer of the panels. Then, tables 2 summarize the results of the efficiency, for each model in the PV emulator.

From these figures, we remark that, for the electrical circuit models and the five lines model, the simulated values agree with the datasheet. For the two lines model they are literally identical at the three calculated points of the (current-voltage) characteristic: The short-circuit current $(0V, I_{sc})$, the open-circuit voltage $(V_{oc}, 0A)$ and the maximum power point (V_{mpp}, I_{mpp}). However, the accuracy is quite low in the other points.

A statistical analysis is required in order to verify the quality of each model. For that reason, we calculated relative error and the mean absolute percentage error (MAPE).

The mean absolute percent error is an indicator of the quality of a linear regression. It helps to measure, in percentage terms, the size of the error. It is calculated by taking into account the relative error (e), according to the equation (21):

$$e = \frac{I_{measured} - I_{calculed}}{I_{measured}} \qquad (20)$$

$$MAPE = \left(\frac{1}{N}\sum_{i=1}^{N}|e_i|\right)\times 100 \qquad (21)$$

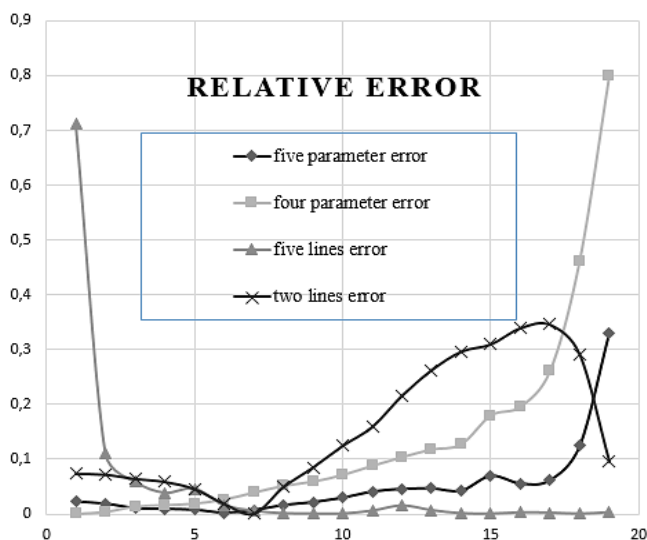Fig 9, shows the relative error (equation (20)) for measurements taken at T=50°C.

Fig. 9. Comparison between relative errors of mathematical and multiple straight lines models

TABLE II
MEAN ABSOLUTE ERROR (MAE) BASED ON THE EXTRACTED PARAMETERS

Model	Five parameter	Four parameter	Five lines	Two lines
MAPE	4,14%	11,39%	5,16%	12,53%

Fig 9 and Table 2 show the relative errors and the MAE of each model. An optimal model must guarantee a minimum of error. The comparison of static analysis results approved that the five parameter and the five-lines models have the most efficiency on the emulator proposed based on buck-boost converter (MAE= 4.14% for the five parameter method), and (MAE= 5.16% for the five-lines model).

The dynamic response of the emulator was another criterion that we considered in the evaluation of the proposed models. Therefore, the dynamic response was calculated for the five parameter and the five lines models, for various solar irradiance and temperature. The load resistance was set to a constant (20Ω) during each state of the simulation. The result for the five parameter model is presented in figure 10 while the result of five lines model is shown in figure 11. The irradiation and temperature levels are shown in the same figures.

Simulations show that the the output voltage of the emulator (V_{pv}) reached the reference voltage (V_{ref}) in 0.008 second, for the two models. Also, the maximum ripple and the waveform on the output voltage are matching in both models.

The last criterion that we considered in the evaluation of the proposed models is the realization economy. The study is based on the component used to execute these commands which will be in our case the microcontroller. The price of microcontrollers depends on their power and memory. Therefore, as an economic study, the decision must be taken for the model which requires simple and reduced calculations, because of the memory limitation of low cost micro-controllers.

According to the different evaluation criteria, the most effective method for modeling a photovoltaic emulator is the five lines model. It presents an optimum model that requires basic and uncomplicated calculations.

IV. CONCLUSION

This paper discusses the modeling, conception and simulation of a photovoltaic emulator based on buck-boost converter. The aim of the developed emulator is to emulate the solar PV characteristics using an accurate mathematical model.

The four developed methods on this paper have been validated by simulation using MATLAB SIMULINK. The different results obtained shows that the developed models represent the curves of the constructors with high accuracy using the proposed emulator.

A comparative study has been done based on the mean absolute error, the response time and the cost, in order to conclude the efficiency of each modeling method. It was found that the five lines method is the most accurate; it performs better according to the theoretical curve and presents an optimum model to use with low cost micro-controllers.
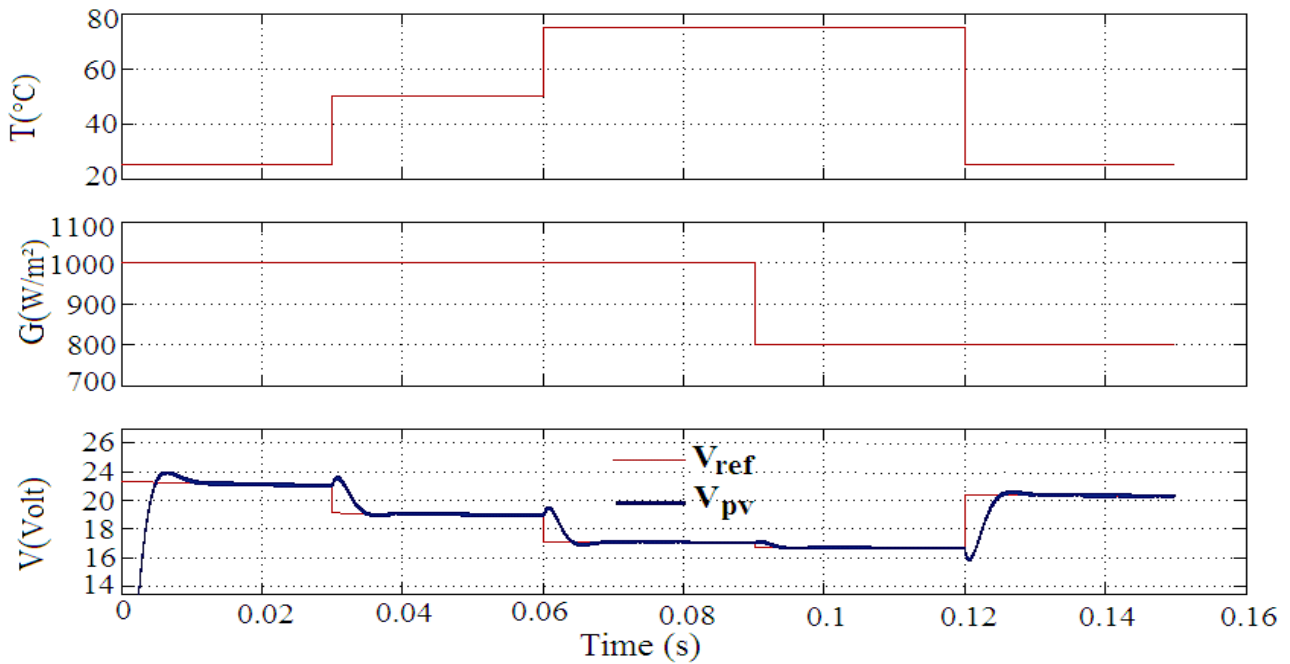
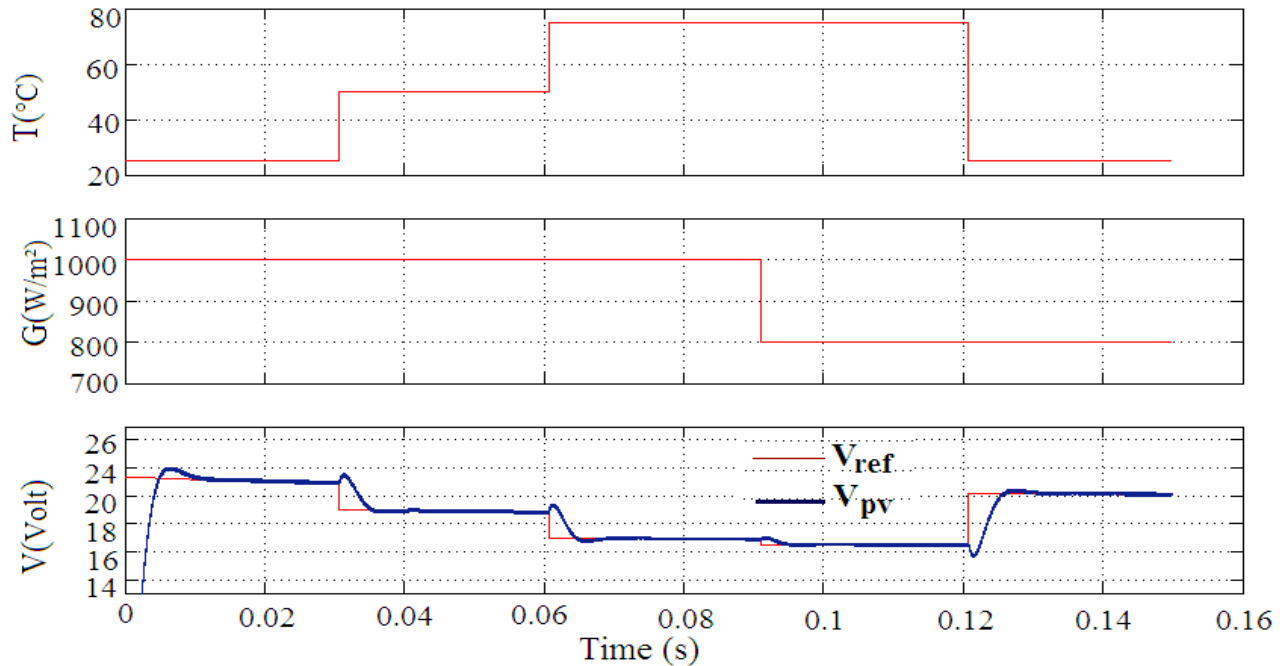Figure. 10. Output characteristics of the emulator for five parameter model

Figure. 11. Output characteristics of the emulator for five lines model

REFERENCES

[1] L. Hernández-callejo, S. Gallardo-saavedra, and V. Alonso-gómez, "A review of photovoltaic systems : Design , operation and maintenance," *Sol. Energy*, vol. 188, pp. 426–440, 2019.

[2] T. Schinko, S. Bohm, N. Komendantova, E. M. Jamea, and M. Blohm, "Morocco ' s sustainable energy transition and the role of financing costs : a participatory electricity system modeling approach," *Energy. Sustain. Soc.*, vol. 8, pp. 1–17, 2019.

[3] K. Choukri, A. Naddami, and S. Hayani, "Renewable energy in emergent countries : lessons from energy transition in Morocco," *Energy, Sustain. Soc. 7(1)*, 2017.

[4] W. Hoffmann, "PV Solar Electricity Industry : Market Growth and Perspective," *Sol. Energy Mater. Sol. Cells*, vol. 90, no. 18–19, pp. 3285–3311, 2006.

[5] O. Oussalem *et al.*, "Realization of a control platform of a photovoltaic system optimized by MPPT strategy 'perturb and observe,'" *Int. Rev. Autom. Control*, vol. 12, no. 3, pp. 115–122, 2019.

[6] D. Abbes, A. Martinez, G. Champenois, and B. Robyns, "Real time supervision for a hybrid renewable power system emulator," *Simul. Model. Pract. Theory*, vol. 42, pp. 53–72, 2014.

[7] S. Jenkal, M. Kourchi, A. Rachdy, M. Ajaamoum, O. Oussalem, and H. Idadoub, "Design and implementation of an agilent-based platform for PV feature generator based on LUT tables," *Mater. Today Proc.*, vol. 24, pp. 95–99, 2020.

[8] M. Ajaamoum, M. Kourchi, B. Bouachrine, A. Ihlal, and L. Bouhouch, "Photovoltaic panel emulators, design and implementation using rapid prototyping technique," *(I.R.E.E.)*, vol. 9, no. 5, pp. 1012–1020, 2014.

[9] C. H. Balakishan and N. Sandeep, "Development of a Microcontroller Based PV Emulator with Current Controlled DC-DC Buck Converter," *Int. J. Renew. Energy Res.*, vol. 4, no. 4, pp. 1049–1055, 2014.

[10] J. Ramos-Hernanz *et al.*, "Two photovoltaic cell simulation models in Matlab/Simulink," *Int. J. Tech. Phys. Probl. Eng.*, vol. 4, no. 1, pp. 45–51, 2012.

[11] E. Manuel, G. Rodrigues, R. Godina, and M. Marzband, "Simulation and Comparison of Mathematical Models of PV Cells with Growing Levels of Complexity," *Energies*, vol. 11, 2018.

[12] M. Ajaamoum, M. Kourchi, B. Bouachrine, M. Oubella, A. Ihlal, and L. Bouhouch, "International Review on Modelling and Simulations (IREMOS), Vol 12 , No 5 Rapid Prototyping Test Bed of MPPT Photovoltaic Controller Based on Takagi-Sugeno Fuzzy Models," *Int. Rev. Model. Simulations*, vol. 12, no. 5, 2019.

[13] R. Szabo and A. Gontean, "Photovoltaic Cell and Module I-V Characteristic Approximation Using Bézier Curves," *Appl. Sci.*, vol. 8, no. 5, p. 655, 2018.

[14] H. Can, "Model of a photovoltaic panel emulator in MATLAB-Simulink," *Turkish J. Electr. Eng. Comput. Sci.*, vol. 21, no. 2, pp. 301–308, 2013.

[15] M. U. Siddiqui and M. Abido, "Parameter estimation for five- and seven-parameter photovoltaic electrical models using evolutionary algorithms," *Appl. Soft Comput. J.*, vol. 13, no. 12, pp. 4608–4621, 2013.

[16] S. Vergura, "A complete and simplified datasheet-based model of pv cells in variable environmental conditions for circuit simulation," *Energies*, vol. 9, no. 5, 2016.

[17] M. G. Villalva, J. R. Gazoli, and E. R. Filho, "Comprehensive Approach to Modeling and Simulation of Photovoltaic Arrays," *IEEE Trans. POWER Electron.*, vol. 24, no. 5, pp. 1198–1208, 2009.

[18] F. R. Quintela, R. C. Redondo, N. R. Melchor, and M. Redondo, "A General Approach to Kirchhoff ' s Laws," vol. 52, no. 2, pp. 273–278, 2009.

[19] M. Hasnaoui, A. Bennani-Ben Abdelghani, and I. Slama-Belkhodja, "Implementation of a PV Panel Model based on the Look-up Tables Method for a PV Generator Emulator," in *Proceedings of the International Conference on Recent Advances in Electrical Systems, Tunisia,* 2016, pp. 290–295.

[20] J. Gonzalez-llorente, D. C. Bogotá, L. A. Garcia-rodriguez, C. Juan, and E. I. Ortiz-rivera, "Simple and Efficient Low Power Photovoltaic Emulator for Evaluation of Power Conditioning Systems," *2016 IEEE Appl. Power Electron. Conf. Expo.*, pp. 3712–3716, 2016.

[21] T. D. Mai, S. De Breucker, K. Baert, and J. Driesen, "Reconfigurable emulator for photovoltaic modules under static partial shading conditions," *Sol. Energy*, vol. 141, pp. 256–265, 2017.

[22] A. Castillo Atoche, J. Vázquez Castillo, J. Ortegón-Aguilar, R. Carrasco-Alvarez, J. Sandoval Gío, and A. Colli-Menchi, "A high-accuracy photovoltaic emulator system using ARM processors," *Sol. Energy*, vol. 120, pp. 389–398, 2015.

[23] I. Moussa, A. Khedher, and A. Bouallegue, "Design of a Low-Cost PV Emulator Applied for PVECS," *Electronics*, vol. 8, no. 2, p. 232, 2019.

[24] M. C. Di Piazza and G. Vitale, "Photovoltaic Sources," 2013, pp. 76–86.

[25] K. Amini, F. Rostami, and G. Caristi, "An efficient Levenberg – Marquardt method with a new LM parameter for systems of nonlinear equations," *Optimization*, vol. 1934, pp. 1–15, 2018.

[26] D. D. C. Lu and Q. N. Nguyen, "A photovoltaic panel emulator using a buck-boost DC/DC converter and a low cost micro-controller," *Sol. Energy*, vol. 86, no. 5, pp. 1477–1484, 2012.